Supporting Information

Wang et al. 10.1073/pnas.0912524107

SI Methods

Construction of Knockin Targeting Vectors. In exon 5 of the mouse *Pten* gene, codon TGT for Cys-124 or codon GGA for Gly-129 was mutated to CGT encoding Arg or GAA encoding Glu, respectively, by means of site-directed mutagenesis. These single-nucleotide changes are found in patients who have Cowden syndrome. Floxed phosphoglycerate kinase promoter (PGK)-*neo* gene was inserted in intron 4 at the site of 295 nucleotides before the start of exon 5. Standard cloning techniques were used to construct targeting vectors. The two arms of homology used for recombination included a 2-kb fragment upstream of the neo cassette and a 4.5-kb fragment downstream of the neo cassette. All the final targeting vectors were confirmed by direct DNA sequencing.

Generation of $Pten^{C124R/+}$ and $Pten^{G129E/+}$ Knockin Mice. TC1 129Sv/Ev ES cells were electroporated with 50 μg of NotI-linearized targeting vectors. Homologous recombination was selected with G418 and FIAU (ganciclovir), confirmed by Southern blot analysis of genomic DNA digested by PvuII, and probed using A and B external probes. Probe A is a PCR product using 5′ primer: 5′-TCCACTGTGGTAGACTAGTCGGTA-3′ and 3′ primer: 5′-TACATATTAGTGGGGTCAGAAGCA-3′. Probe B is amplified using 5′ primer: 5′-ACCTAAAGCAGAATCCTTATGTGT-3′ and 3′ primer: 5′-GAATTCTGATCACTACAGTTCACTTTT-3′. Probes were confirmed by sequencing. ES cell clones carrying the expected *Pten* mutation were injected into E3.5 C57BL/6 blastocysts that were subsequently transferred into foster mothers. The resulting chimeras were bred with National Institutes of Health (NIH) Black Swiss female mice, and agouti offspring were genotyped by PCR and confirmed by Southern blot analysis. Offspring with germline transmission of $Pten^{C124R/+}$ and $Pten^{G129E/+}$ knockin targeted alleles were bred with *EIIA-cre* mice to excise the PGK-neo cassette. Knockin mutation was confirmed by sequencing tail DNA samples from agouti mice.

Genotyping of Knockout and Knockin Mice. Genotyping of offspring was performed by PCR and Southern blot analysis. Southern blot analysis was performed using genomic DNA digested with PvuII and a ^{32}P-labeled probe A or probe B fragment as the hybridization probe. The WT, the $Pten^{C124Rneo}$ and $Pten^{G129Eneo}$ alleles (with the neo cassette), and the $Pten^{C124R}$ and $Pten^{G129E}$ alleles (without the neo cassette) yielded fragments of ∼9.1, 4.75, and 9.1 kb, respectively. Hemizygous MEFs with their respective knockin mutant allele were obtained by deleting a *Pten* floxed allele ($Pten^{LoxP}$) with a retrovirus expressing *cre* in heterozygous MEFs, which contain *Pten* knockin and $Pten^{LoxP}$ alleles. Multiplex PCR genotyping used three primers to detect the knockin (primer 1, primer 2, and primer 3) and knockout (primer 4, primer 5, and primer 6) alleles. PCR to detect $Pten^{LoxP}$, $Pten^{\Delta 4-5}$, $Pten^{C124R}$, and $Pten^{G129E}$ alleles used the following conditions: 94 °C, 3 min; 35 cycles of 94 °C, 30 s; 55 °C, 30 s; 72 °C, 45 s; 72 °C, 3 min. Primers were obtained from Invitrogen, and their sequences are listed in Table S3.

Mouse Breeding Schemes. Mice bred in the same strain background were raised and segregated by genotypes into four groups. These four groups were $Pten^{C124R/+}$, $Pten^{G129E/+}$, $Pten^{\Delta 4-5/+}$, and $Pten^{+/+}$. For embryo analysis, mouse strain background is 50% FVB/N (FVB), 25% 129Sv/Ev, and 25% Black Swiss. All adult mice observed for tumor spectrum analysis have 75% FVB, 12.5% 129Sv/Ev, and 12.5% Black Swiss strain backgrounds.

Generation of MEFs, Retroviral Infections, and Cell Culture Conditions. Primary MEFs were isolated from E13.5 embryos using standard methods. MEFs were cultured in DMEM-15% FBS. For the production of retrovirus, the *cre* cDNA was cloned into pBabe-puromycin. High-titered retroviruses were produced by transient transfection of retroviral constructs into the Phoenix-Eco packaging cell line as described previously (1). MEFs were infected by incubating the cells for 5 h with the supernatants containing 4 μg/mL Polybrene (Sigma-Aldrich) from the transfected cells. Subsequent to infection, cells were split and grown in selection media containing 2.5 μg/mL puromycin (Sigma) for 3–5 days. Introduction of *cre* by virus infection of MEFs resulted in deletion of the floxed WT allele, which was confirmed by genotyping of MEF DNA and Western blot analysis using PTEN antibody.

Protein and RNA Analysis. Cells were scraped from culture dishes in chilled PBS, centrifuged, and washed once with ice-cold PBS. Total protein extracts were prepared by incubating cells in radioimmunoprecipitation assay (RIPA) extraction buffer for 30 min on ice and were measured by Bradford assay. For Pten protein half-life analysis, in vivo stably expressing WT or mutant Pten MEFs were treated with 20 μg/mL cycloheximide in DMEM-15% FBS. Whole-cell protein lysate was extracted at 0, 2, 4, 8, 12, and 24 h after addition of cycloheximide. In total, 30 μg of protein was then separated by 10% SDS/PAGE and transferred to PVDF membranes. Blots were probed with antibodies specific for PTEN (catalog no. 9559, 1:1,000 dilution; Cell Signaling Technology, Inc.), p-Akt (Ser473, catalog no. 4058, 1:1,000 dilution; Cell Signaling Technology, Inc.), and Akt (catalog no. 4685, 1:1,000 dilution; Cell Signaling Technology, Inc.). Anti-α-tubulin (T6199, 1:5,000 dilution; Sigma) was used to determine protein loading. Total RNA was extracted from MEFs using TRIzol following Invitrogen's protocol. Reverse transcription of 5 μg of total RNA was performed by combining 1 μL of SuperScript III reverse transcriptase (Invitrogen, Life Technologies Corp.), 4 μL of 5× buffer, 0.5 μL of 100 μM oligo(dT) primer, 0.5 μL of 25 mM deoxyribonucleotide (dNTP), 1.0 μL of 0.1 M DTT, 1.0 μL of RNase Inhibitor (Roche), and water up to a volume of 20 μL. Reactions were incubated at 50 °C for 60 min and then diluted 5-fold with 80 μL of water. Quantitative RT-PCR was performed using a BioRad iCycler PCR machine. Each PCR contained 0.5 μL of cDNA template and primers at a concentration of 100 nM in a final volume of 25 μL of SYBR green reaction mix (BioRad). Each PCR yielded only the expected amplicon, as shown by the melting temperature profiles of the final products and by gel electrophoresis. Standard curves were generated using cDNA to determine the linear range and PCR efficiency of each primer pair. Reactions were performed in triplicate, and relative amounts of cDNA were normalized to GAPDH. Primer sequences are listed in Table S3.

Histopathology and IHC. Tissue samples were collected and fixed in formalin, 10%, neutral, phosphate buffer. Paraffin-embedded tissues were cut into 4-μm thick sections and then stained with H&E by standard methods. IHC using PTEN (catalog no. 9559L, 1:100 dilution; Cell Signaling Technology, Inc.) or p-Akt S473-specific (catalog no. 3787S, 1:50 dilution; Cell Signaling Technology, Inc.) antibody was performed on paraffin-embedded sections with 3,3′-diaminobenzidine and counterstained with hematoxylin following the manufacturer's protocol.

p-Akt IHC, Laser Capture Microdissection, and LOH Analyses. Formalin-fixed paraffin-embedded sections (8 μm in thickness) containing epithelial cells from lesions in the uterus, thyroid, prostate, and mammary gland were stained using a p-Akt S473-specific antibody with 10 min of antigen retrieval in a steamer, 20 min of primary antibody incubation, 30 min of secondary antibody incubation, and no avidin or biotin blocking treatment. Microdissection of epithelial cells expressing high p-Akt was performed using a PALM ROBO Microbeam laser (Carl Zeiss MicroImaging). DNA was isolated using the QIAamp DNA Micro Kit (catalog no. 56304; Qiagen). LOH of the WT *Pten* allele was measured by PCR using primers 1 and 3 for the knockin heterozygote ($Pten^{C124R/+}$ or $Pten^{G129E/+}$) or using primers 4, 5, and 6 for the knockout heterozygote ($Pten^{\Delta 4-5/+}$). In addition to the capture of cells for DNA, cells for RNA were captured from uterus lesions to perform allelic expression imbalance analysis. These tissues were embedded using Optimal Cutting Temperature solution (Tissue-Tek) and frozen. Frozen 8-μm sections were stained with cresyl violet and eosin following the Laser Capture Microdissected Staining Kit (catalog no. AM1935; Ambion). Epithelial cells within lesions were identified and captured under the supervision of the pathologist. RNA was isolated from these samples using the RNAqueous-Micro Microscale RNA isolation kit (Ambion).

Statistical Analysis. All the tests were two-sided. For the outcome variable of embryo viability (Fig. 2*A*), χ^2 or Fisher's exact tests were used to compare the observed and expected number of deaths for each genetic group. Fisher's exact tests were used when less than five dead embryos were observed. In Fig. 2*C*, the plot shows three tumor categories: 0–1 organ, 2–4 organs, or 5–7 organs. Statistical analyses of all the individual uncategorized data used the Poisson regression model. For Fig. 3 *A–D*, the organ pathological findings were analyzed by χ^2 or Fisher's exact tests. Holm's method was used to adjust for multiple comparisons among genotypes. For Fig. 3*E*, the binomial exact test was used to test the null hypothesis (no tumors) for each genetic group. For Fig. 5*C*, Pten protein stability was analyzed by an ANOVA model with repeated measures (SAS Institute, Inc.). The trend across time points was compared between WT and each *Pten* mutant sample. For Fig. S2, the frequency of lesions in the indicated organs was compared between the two genders within each genotype using the normal approximation method. For Fig. S4*C*, the binomial exact test was used to compare frequencies of male mice of the different genotypes having mammary lesions. For Fig. S6*C*, the two-sample *t* test was used to compare *Pten* gene expression levels between C124R/Δ*4–5* and G129E/Δ*4–5* MEFs. Each bar represents the average mean value obtained from triplicate measurements. Four independent MEF preparations were used for each genotype. For Table S1, χ^2 or Fisher's exact tests were used to compare the number of mice having lesions in each of the indicated organs. Fisher's exact tests were used when the number of affected mice was less than five. For Table S2, χ^2 tests were used to compare the observed vs. expected number of mice that had lesions in the indicated organ pairs within each genotype. The expected proportion of mice having affected organ pairs was obtained by multiplying the affected proportion for each organ (assuming independence between organs). The expected number of mice was obtained by multiplying the expected proportion by the total number of mice. *P* values were not adjusted because this represents an explorative analysis.

Uterus-Endometrium. Endometrial proliferative lesions were classified based on an internationally accepted histological grading system (2). Simple hyperplasia (SH) of endometrium was characterized by a localized increase in the density of endometrial glands with hyperplastic epithelium. Some of the hyperplastic glands were dilated (cystic type). The glands with SH retained normal endometrial stroma. In atypical hyperplasia (AH), the hyperplastic glands were irregularly shaped with loss of intervening stroma. The glands were enlarged with irregular branching and often had a cribriform pattern. The glandular epithelium had features of cytological atypia and loss of polarity. Increased mitotic figures and occasional single-cell necrosis were present. These AH lesions lacked features of myometrial invasion characteristic of endometrial carcinoma.

Thyroid. The proliferative lesions of the thyroid gland were confirmed to be follicular in origin by means of IHC for thyroglobulin. The thyroid follicular proliferative lesions were classified based on a published grading system (3). Follicular hyperplasia was characterized by small nodules of proliferating follicular cells that were well demarcated from the adjacent thyroid parenchyma. The hyperplastic follicular cells often formed small follicles with little or no colloid. Follicular adenoma was distinguished by the presence of well-circumscribed nodules with compression of the adjacent thyroid parenchyma. The adenomas contained a follicular to solid growth pattern. Occasionally, both patterns were present in the same neoplasm. The neoplastic follicular cells were cuboidal to columnar, with features of cytologic atypia.

Prostate. The proliferative lesions of the prostate gland were classified based on a published grading system (4, 5). Briefly, prostate intraepithelial neoplasia (PIN) I lesions had one to two layers of proliferative and atypical cells. PIN II lesions had more than two layers of proliferative and atypical cells with a distinct protrusion toward the lumen. PIN III lesions had large foci of proliferative and atypical cells that almost filled the lumen of the glands. PIN IV lesions had irregular bulging of the glands with proliferating cells filling and focally expanding glands and ducts. In PIN IV lesions, mild periductular fibrovascular proliferation and mild foci of necrosis were occasionally present. Prostate carcinomas were distinguished from PIN IV lesions by the presence of invasive finger-like projections or single tumor cells protruding into the periglandular hypercellular fibrovascular stroma (desmoplasia). The carcinomas also had increased cytological atypia, mitoses, necrosis, and infiltration of inflammatory cells.

Mammary Gland. The proliferative lesions of the mammary gland were classified according to a published grading system (6). MIN was characterized by intraluminal epithelial proliferative lesions with cytological and nuclear atypia. Low-grade MIN had more than one layer of atypical epithelial cells (luminal and/or myoepithelial cells) containing little cytoplasm, with nuclear crowding and an increased mitotic rate. High-grade MIN had more than two layers of atypical epithelial cells that almost filled the lumens of ducts and had increased pleomorphism of nuclei and/or epithelial cells, greater numbers of mitoses, and an intact basement membrane. The mammary carcinomas were characterized by proliferation of atypical mammary epithelial cells with stromal invasion along the tumor margins. The carcinomas were frequently surrounded by hypercellular stroma (desmoplasia) with abundant extracellular matrix. Some of the mammary carcinomas were adenosquamous variants with areas of squamous differentiation.

1. Pear WS, Nolan GP, Scott ML, Baltimore D (1993) Production of high-titer helper-free retroviruses by transient transfection. *Proc Natl Acad Sci USA* 90:8392–8396.
2. Scully RE, et al. (1994) *Histological Typing of Female Genital Tract Tumours (International Histological Classification of Tumours)* (Springer, New York), 2nd Ed.
3. Robert RM (1999) *Pathology of the Mouse: Reference and Atlas* (Cache River Press, Vienna, IL), 1st Ed.
4. Park JH, et al. (2002) Prostatic intraepithelial neoplasia in genetically engineered mice. *Am J Pathol* 161:727–735.

5. Shappell SB, et al. (2004) Prostate pathology of genetically engineered mice: Definitions and classification. The consensus report from the Bar Harbor meeting of the Mouse Models of Human Cancer Consortium Prostate Pathology Committee. *Cancer Res* 64:2270–2305.

6. Cardiff RD, et al. (2000) The mammary pathology of genetically engineered mice: The consensus report and recommendations from the Annapolis meeting. *Oncogene* 19: 968–988.

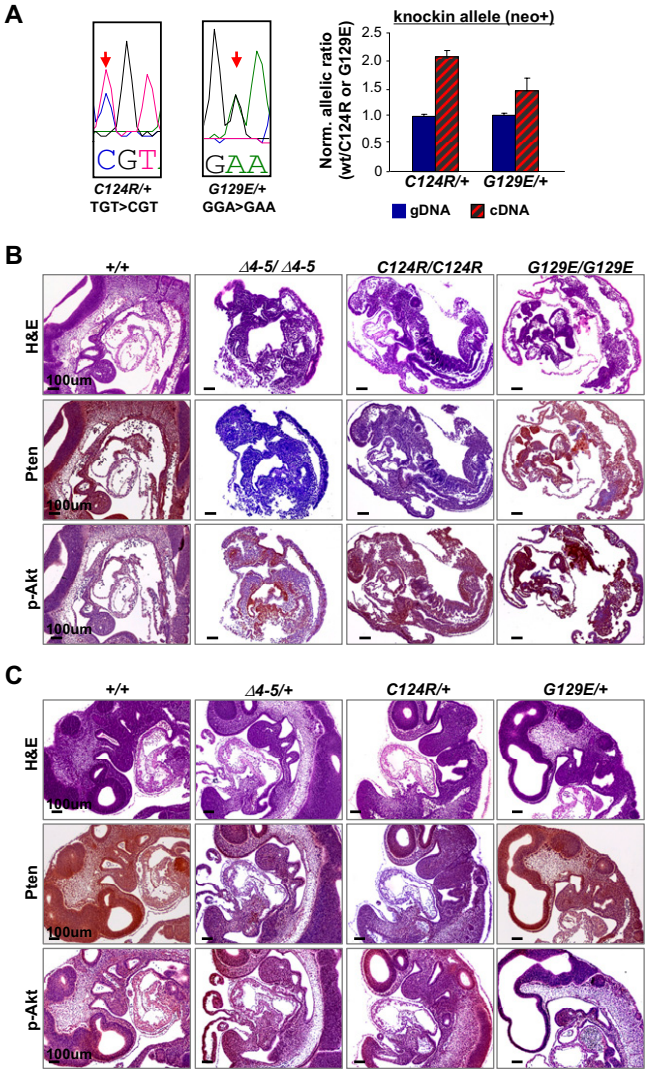

Fig. S1. Verification of point mutations of *Pten* alleles and histopathological (H&E) and IHC staining of Pten and p-Akt S473 embryos at E9.5. (A) (*Left*) Sequence analysis of tail DNA isolated from $Pten^{C124R/+}$ and $Pten^{G129E/+}$ mice. Chromatograms show the successful mutations (C124R and G129E) in the targeted *Pten* locus. Arrows point to targeted nucleotides. (*Right*) Allelic expression imbalance analysis of allele-specific expression. The graph shows the proportion of mRNA expressed from the WT allele over the indicated mutant allele in lungs of $Pten^{C124R/+}$ and $Pten^{G129E/+}$ mice. neo+, mice containing the PGK-neo cassette. Genomic DNA (gDNA) was used as an internal control. (*B* and *C*) Histopathological (H&E) and IHC staining of Pten and p-Akt S473 embryos at E9.5. (*B*) Homozygous mutant embryos of the three genetic groups had similar developmental defects. The development of mutant embryos that were obtained at E9.5 was severely compromised, with defects in anterior-posterior patterning, failure of axial rotation, and absence of overt tissue differentiation leading to resorption. (*C*) Heterozygous embryos of the three genetic groups were morphologically normal.

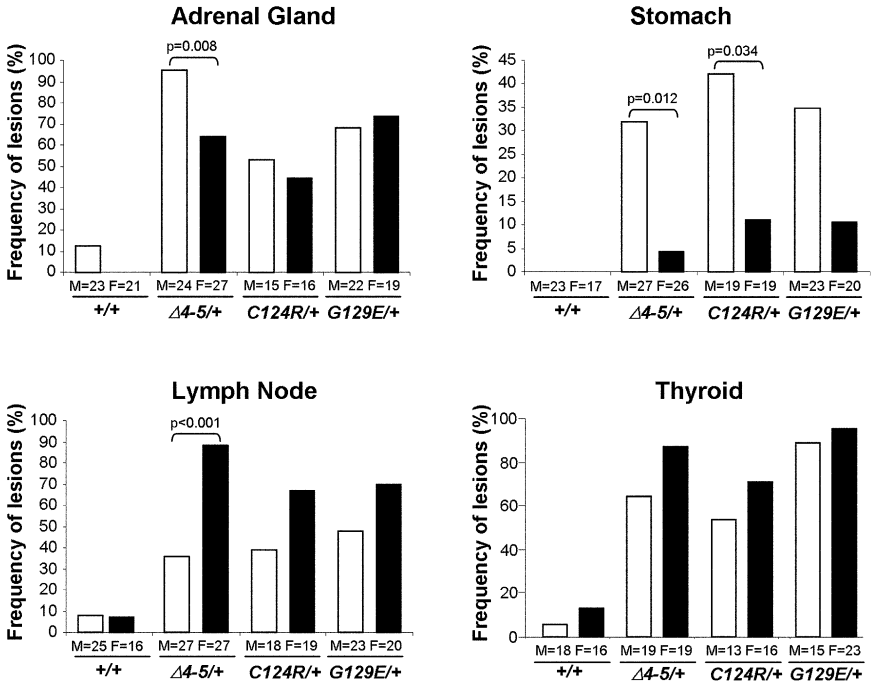

Fig. S2. Incidence of proliferative lesions in the adrenal, stomach, lymph node, and thyroid varies by gender. Male (M) and female (F) mice were observed during their first 9 months of life for the incidence of proliferating lesions; at that time, they were killed and a necropsy was performed. The frequency of lesions in the indicated organs of male and female mice was analyzed by the normal approximation method; significant differences are shown.

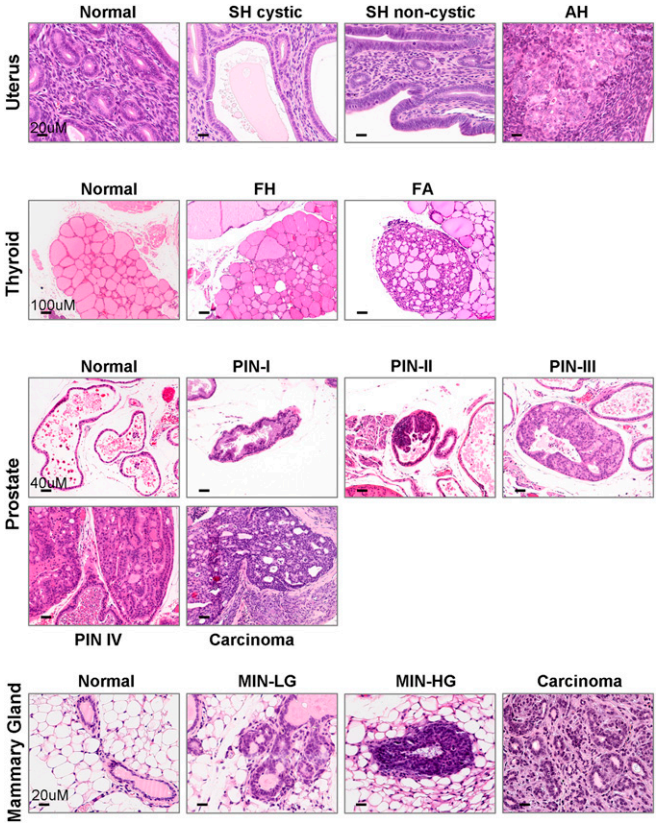

Fig. S3. Consensus among a panel of pathologists (S.N., P.S., K.L.P., and T.R.) was achieved on the selection and implementation of a standardized histopathological grading system. Salient descriptive features of various grades of lesions identified in the uterus, thyroid, prostate, and mammary gland are shown in *SI Methods*.

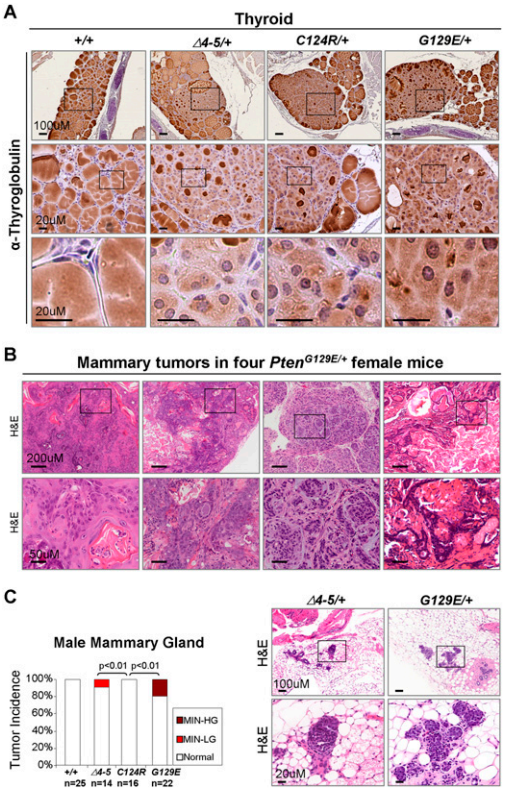

Fig. S4. (*A*) Thyroglobulin IHC staining of thyroid proliferative lesions confirmed that the proliferating cells were of follicular cell origin in all genetic groups. (*Upper*) Lesions shown here are follicular adenomas from 9-month-old heterozygous mutant mice. (*Lower*) Enlarged views of the corresponding upper panels. (*B*) $Pten^{G129E/+}$ heterozygous females developed palpable mammary tumors at ~12–15 months of age (n = 4). (*Upper*) Mammary tumors in the four mice had histological characteristics of invasive carcinoma replacing >50% of the mammary fat pads. (*Lower*) Enlarged views of the corresponding black boxes in the upper panels. (*C*) Mammary tumors developed only in $Pten^{G129E/+}$ and $Pten^{\Delta4-5/+}$ male mice. (*Left*) Tumor incidence in mammary glands of 4- and 9-month-old (combined) male mice. The frequency of lesions in the various genetic groups was evaluated by the exact binomial test. (*Right*) H&E images of the highest grade mammary lesions observed in male mammary glands of the indicated genotypes. (*Lower*) Enlarged views of boxed areas in upper panels.

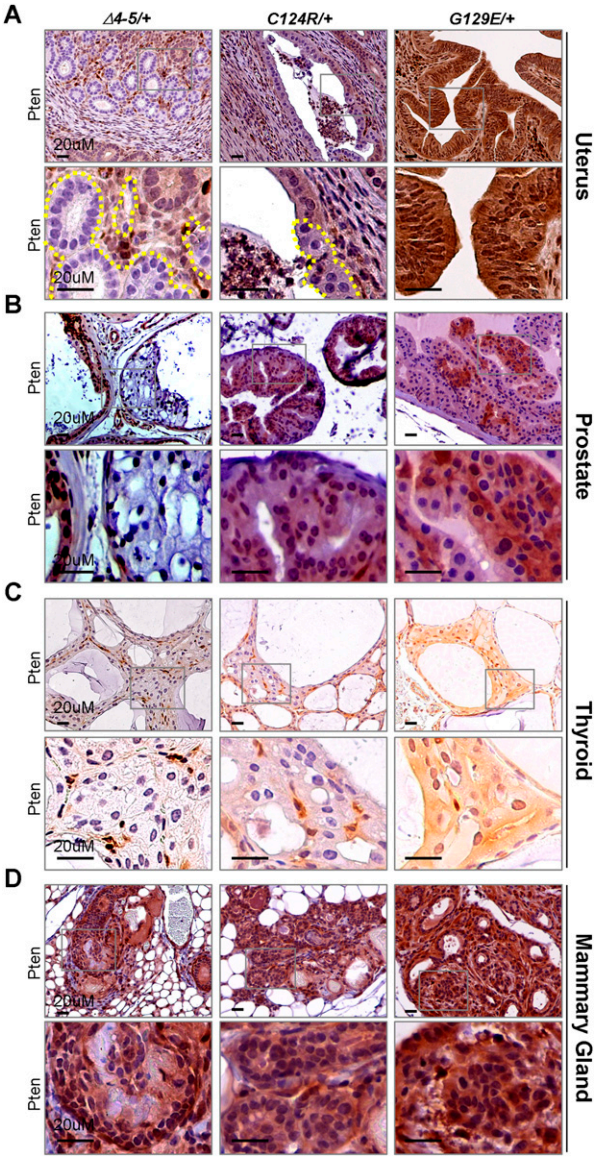

Fig. S5. Loss of Pten was observed in early stages of the proliferative lesions in the uterus, prostate, and thyroid gland from $Pten^{\Delta 4-5/+}$ as well as $Pten^{C124R/+}$ mice but not in early-stage lesions of the mammary gland from any mutant mice. Pten expression was observed in early lesions of all four $Pten^{G129E/+}$ organs. In some areas of proliferative prostate lesions, high Pten expression was observed in $Pten^{G129E/+}$ groups. (*Lower*) Enlarged views of boxed areas in upper panels.

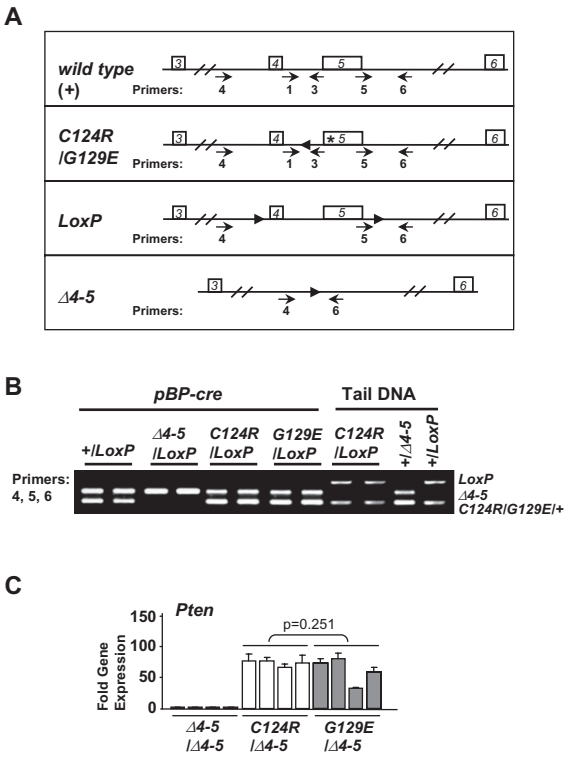

Fig. S6. (*A*) Schematic representation of the various *Pten* alleles. PCR primers used to detect each allele are indicated. (*B*) PCR analysis of *cre*-mediated deletion of the $Pten^{LoxP}$ allele. (*C*) Quantitative RT-PCR analyses show similar levels of $Pten^{C124R}$ and $Pten^{G129E}$ mRNA expression. The two-sample *t* test was used to compare gene expression levels between the $Pten^{C124R/\Delta4\text{-}5}$ and $Pten^{G129E/\Delta4\text{-}5}$ groups.

Table S1. Distribution of proliferative lesions in *Pten* mutant mice

	+/+		Δ4–5/+			C124R/+			G129E/+		
	%	*n*	%	*n*	*P**	%	*n*	*P**	%	*n*	*P**
Uterus	56.2	16	94.4	18	0.014	71.4	14	0.460	80.9	21	0.151
Thyroid	8.8	34	76.3	38	<0.00	58.6	29	<0.00	81.6[‡]	38	<0.001
Prostate	50.0	18	93.3	15	0.009	73.3	15	0.284	86.4	22	0.018
Breast, female	11.1	18	57.9	19	0.005	20.0*	15	0.693	55.0[§]	20	0.006
Breast, male	0.0	15	10.0	10	0.400	0.0	11		11.1	18	0.489
Adrenal gland	4.5	44	76.5	51	<0.00	51.6[†]	31	<0.001	70.7	41	<0.001
Lymph node	7.3	41	58.9	54	<0.00	54.1	37	<0.001	55.8	43	<0.001
Thymus	6.2	32	55.8	52	<0.00	65.0	29	<0.001	59.5	37	<0.001
Stomach	10.0	40	17.0	53	0.382	26.3	38	0.079	23.3	43	0.145
Intestine	2.3	44	19.1	47	0.016	3.6	28	0.999	4.4	23	0.999

The three *Pten* mutant groups of mice developed a similar pattern of proliferative lesions as in patients with Cowden syndrome. The table shows the incidence of proliferative lesions in organs at 9 months. %, percentage of mice in each genetic group with proliferative lesions; *n*, total number of mice examined; *P**, *P* value comparing the indicated *Pten* mutant and WT groups. Fisher's exact or χ^2 or tests were used to compare the frequency of mice with lesions as described in *SI Text*.
*(*P* = 0.038) and [†](*P* = 0.020) represent the *P* value comparing the *C124R*/+ and *Δ4–5*/+ groups; [‡](*P* = 0.039) and [§](*P* = 0.046) represent the *P* value comparing the *G129E*/+ and *C124R*/+ groups.

Table S2. Coexisting lesions in paired organs of *Pten* mutant mice

	Δ4–5/+			C124R/+			G129E/+		
	Obs.	Tot.	*P**	Obs.	Tot.	*P**	Obs.	Tot.	*P**
Breast, female/Intestine				1	15	0.007			
Breast, female/Adrenal				4	15	0.049			
Breast, female/Lymph node	15	19	0.001				11	20	0.050
Uterus/Lymph node	18	20	0.032						
Thyroid/Lymph node	28	38	0.003						
Prostate/Stomach	6	15	0.003	6	15	0.002			

Only significant organ pairs are reported for each genotype. To compare the observed vs. expected number of mice that have lesions in the indicated organ pairs within each genotype, χ^2 tests were used. Obs., observed number of mice that have lesions in the indicated organ pairs; *P**, *P* value represents the association between organ pairs within each genetic group; Tot., total possible number of mice with the indicated organ pair.

Table S3. Primers for genotyping and quantitative RT-PCR

Gene	Forward primer		Reverse primer	
Genotyping				
$Pten^{C124R/G129E}$	Primer 1	TTCTTCGGAGCATGTCTGG		
	Primer 2	GGGGGAACTTCCTGACTAGG	Primer 3	CATGGAAACAAGCATTGTGC
$Pten^{LoxP/\Delta4-5}$	Primer 4	GAATGATAATAGTACCTACTTCAG		
	Primer 5	GAATGCCATTACCTAGTAAAGCAAGG	Primer 6	CATGGAAACAAGCATTGTGC
EIIA-cre	Primer 7	ATGCTTCTGTCCGTTTGCCG	Primer 8	CCTGTTTTGCACGTTCACCG
qRT-PCR for gene expression assays				
Pten	Primer 9	TTGACCAATGGCTAAGTGAAGA	Primer 10	TATACATAGCGCCTCTGACTGG
GAPDH	Primer 11	CGGTGTGAACGGATTTGGC	Primer 12	TTTGATGTTAGTGGGGTCTCGC

Sequences of the forward and reverse primers are listed for genotyping (primer sequences 1–8) and quantitative RT-PCR (primer sequences 9–12).